Error analysis of quantitative precipitation estimates from NCAS's X-band polarimetric radar.

David Dufton

David Dufton[1,2], Lindsay Bennett[1,2], and Chris. Collier[1,2]

[1]*National Centre for Atmospheric Science, University of Leeds, Leeds, LS2 9JT, UK*
[2]*School of Earth and Environment, University of Leeds, Leeds, LS2 9JT, UK*
(Dated: 17 July 2014)

1. Introduction

Dual polarisation weather radars provide significantly more information about the observed scan volume than conventional weather radars. This additional information offers increased capability for dynamic processing of radar returns leading to more accurate quantitative precipitation estimates (QPE). The deployment of the National Centre for Atmospheric Science (NCAS) mobile polarimetric Doppler X-band radar during the COnvective Precipitation Experiment (COPE) presents a new opportunity for developing these processing techniques prior to future deployments of the radar.

The NCAS radar was deployed during the COPE field campaign in Cornwall, south-west England (Figure 1). The NCAS radar operates with a one degree beamwidth, and during the field campaign had a range gate length of 150m out to 150km range. More information about the radar and the wider campaign can be found in Collier et al. (2014) and at www.ncas.ac.uk/cope. Within 50 kilometres of the radar were 20 tipping bucket rain gauges operated by the Environment Agency, while one operational C-band radar from the UK Met Office network at Cobbacombe Cross was located within 100km of the NCAS radar . Data from both these sources have been used to analyse the QPEs obtained from the NCAS radar.

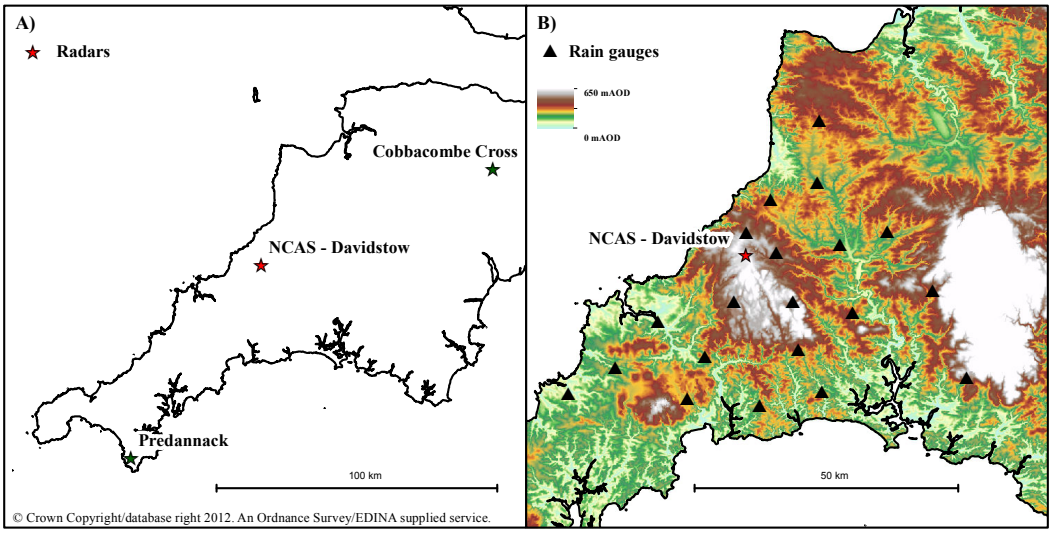

Figure 1: A) Location of the COPE field campaign in south-west England (red star), including the location of the UKMO network radars (green stars). Unfortunately the Predannack radar was out of service during the field campaign. B) Terrain in the area around Davidstow airfield, with the locations of the Environment Agency rain gauges used in this study.

2. Identification of radar QPE errors

Ground clutter is just one of a plethora of known radar error sources which also include partial beam blockage, attenuation and fixed retrieval functions (Villarini and Krajewski, 2010). These error sources combine to produce a wide uncertainty range for radar QPEs. Figure 2 illustrates this by presenting a comparison of rainfall obtained from raw reflectivity measurements (converted using the Marshall Palmer relation (Marshall and Palmer, 1948)) to ground observations from the rain gauges across the Cornish peninsula.

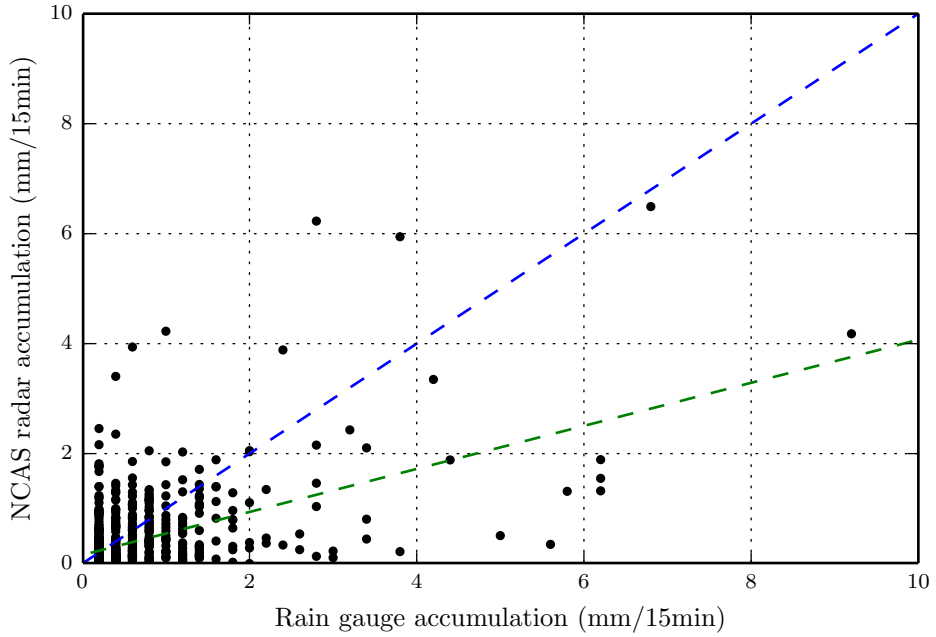

Figure 2: Comparison of raw radar measurements with rain gauge observations. The green line indicates a linear fit between the points with gradient=0.39 and correlation=0.55, the blue line shows the 1:1 relationship.

While some radar errors are obvious at the moment of retrieval, such as the attenuation seen in Figure 3, the majority are predicted prior to installation using ground survey information and beam physics, or identified after a period of observational data has been collected using data comparison and summary statistics. In the cases of ground clutter and partial beam blockage both methods can be utilised and allow the production of static identification maps which can be applied to future scans, or retrospectively. Figure 4 shows that clear regions of ground clutter returns and beam blockage can be identified for the Davidstow airfield site using a summation across the data collection period of the COPE campaign. The strong beam blockage at 305° visible at both elevations is a result of the airfield control tower, while other beam blockage from high topography is visible at the lowest elevation in the 120° to 200° sector. Also visible are speckles from radar interference (at 221°, 104km, in the 0.5° scan for example) which produce extreme reflectivity values in signal scans high enough to pollute a simple summation such as this,

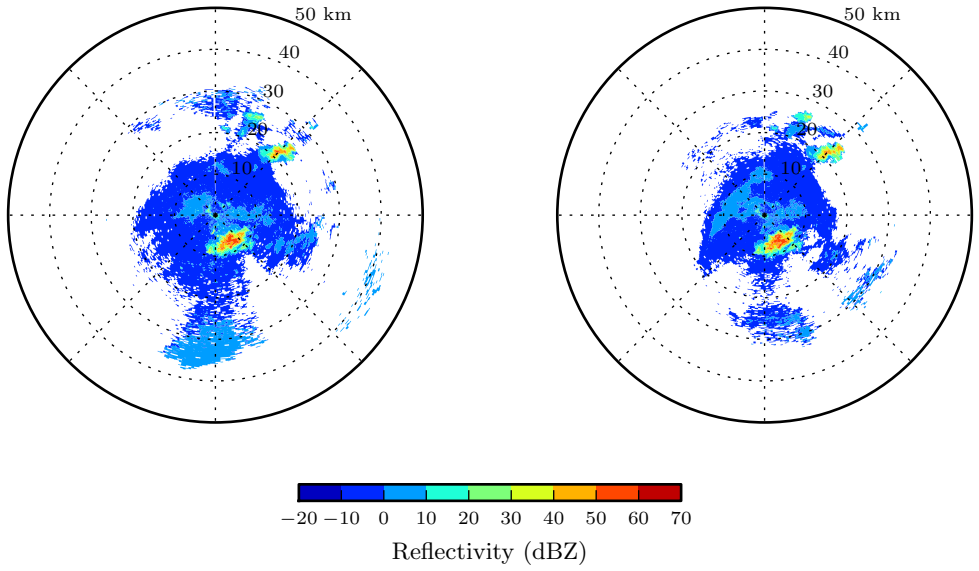

Figure 3: 18th July 2013 volume scan, showing signal attenuation clearly in the reflectivity field from both the 1.5° (left plot) and 2.5° (right plot) elevation scans due to the intense storm cell within 10km of the radar at 140° azimuth.

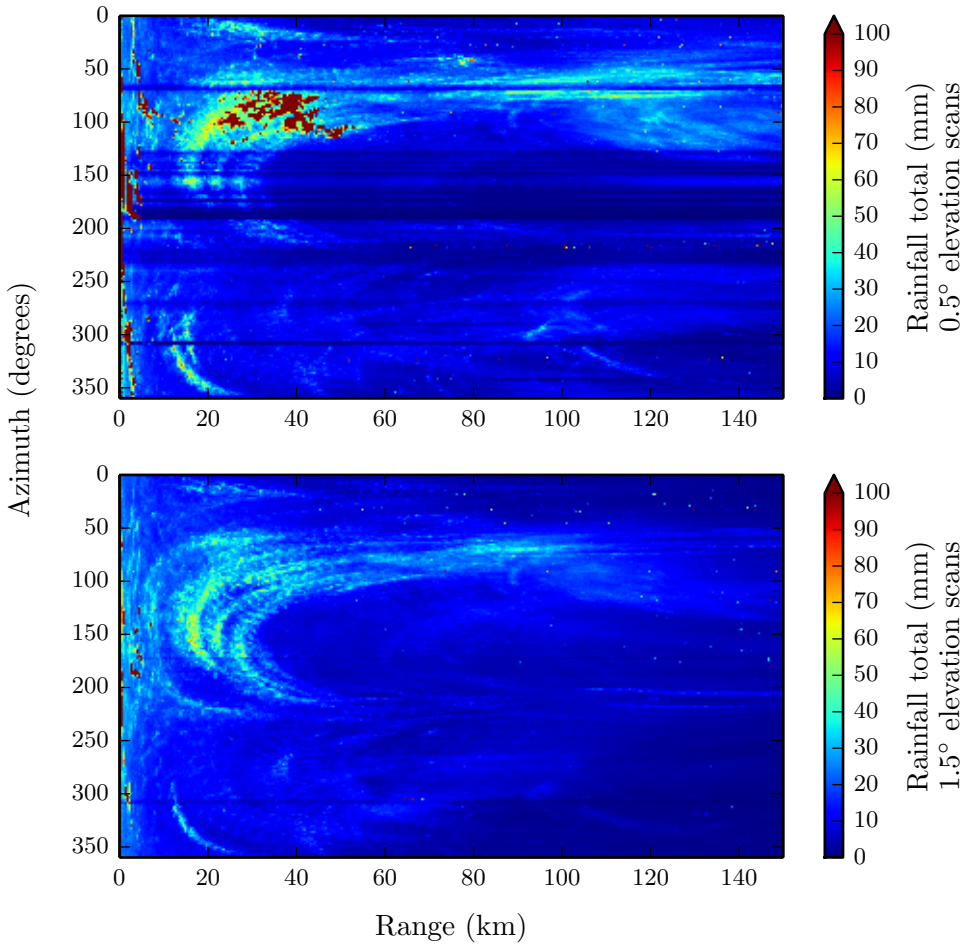

Figure 4: Total observed rainfall from all scans during the COPE field campaign, at 0.5° and 1.5° elevation, assuming $Z=200R^{1.6}$ and backwards projection between scans to calculate the accumulation over time. The maximum total for the 0.5° elevation is 39121.4mm and for the 1.5° elevation is 15185.4mm.

Another prominent feature in Figure 4 is the near field ground clutter located within ten kilometres of the radar and present in both scans, shown by the extreme 'rainfall' totals. These extremes also highlight the effect of the Dartmoor area of high topography at around 40km range, 90° azimuth in the 0.5° scan.

While filtering the static elements of ground clutter using basic analysis is possible, the effects of anomalous propagation providing variability in the clutter field requires more complex processing. Techniques used have included statistical comparison to satellite retrievals (Harrison et al., 2000) and multi stage decision trees (Germann et al., 2006). Dual polarisation also allows for a dynamic approach to identification of ground clutter.

3. Dynamic ground clutter removal

In the present paper dual polarisation variables have been used to identify clutter. Clutter identification, and more widespread hydrometeor classification, has been developing rapidly with the increasing use of dual polarisation radars, with the majority of classification schemes being focused on S-band systems (Chandrasekar et al., 2013). Recently schemes for X-band radars have also been developed, such as the theoretical scheme developed by Dolan and Rutledge (2009) or empirical schemes like that proposed by Gourley et al. (2007). Both of these schemes use fuzzy logic membership sets to define the classification scheme. Fuzzy logic has been used in the work reported here, with the use of an empirical approach for development of the fuzzy set membership functions. For the classification scheme the following radar parameters were used:

- Coefficient of correlation between horizontal and vertical phase (ρ_{hv})
- Radial texture of reflectivity
- Radial texture of differential reflectivity

- Radial texture of differential phase shift

Radial textures were calculated using equation 3.1 which defines the standard deviation of the sample along a linear window of length N, centred on the range gate located at azimuth α and range r. In this study N was set to 7, which equates to a window size of 1050 metres by one degree. Future work will test this definition against more traditional two dimensional window textures.

$$\sigma(x_{\alpha,r}) = \sqrt{\frac{1}{N-1}\sum_{i=r-\frac{N-1}{2}}^{N}(x_{\alpha,i}-\bar{x})^2} \tag{3.1}$$

Prior to developing the classification parameters, it was also necessary to correct for the increasing value of texture parameters with range, as demonstrated by Gourley et al. (2007). A third order polynomial multiplicative correction factor was applied to both the texture of differential reflectivity and the texture of phase shift at a range beyond 25km, which was calculated using an empirical fit to the average trend observed over five, 1.5° elevation, scans on the 17th August 2013.

Classification histograms of observed variables for both rainfall and ground clutter were produced using masked regions at 1.5° elevation for rainfall, and 0.5° elevation for ground clutter, from one hour of data (12 scans) on the 5th August 2013. A Gaussian KDE was then fitted to the observations, and its triangular approximation used to define the fuzzy membership functions as shown in equation 3.2.

$$M(x)_j = \begin{cases} 0 & \text{if } x_j \leq a_j \text{ or } x_j \geq c_j \\ \frac{1}{b_j - a_j} \times (x_j - a_j) & \text{if } a_j < x_j < b_j \\ \frac{-1}{c_j - b_j} \times (x_j - b_j) & \text{if } b_j < x_j < c_j \end{cases} \tag{3.2}$$

Here a, b and c are the variable lower limit, peak and upper limit of the fuzzy set.

$$F(x) = \sum_{j=1}^{4} M(x)_j \times W_j \tag{3.3}$$

The total membership score for each variable (j) is defined by the additive equation 3.3, where W_j is the variable weight. Table 1 shows the parameters used in this study for both ground clutter and rainfall.

Table 1: Empirically defined fuzzy membership parameters.

Ground Clutter				
Parameter	a_j	b_j	c_j	W_j
σ_{ZDR}	-0.2	1.5	8	1
σ_{Z_H}	5	20	35	1
$\sigma_{\phi_{dp}}$	-10	25	150	1
ρ_{HV}	0	0.94	1.05	1

Rainfall				
Parameter	a_j	b_j	c_j	W_j
σ_{ZDR}	0	0.22	1.22	1
σ_{Z_H}	0	2	6	1
$\sigma_{\phi_{dp}}$	-3	2.5	12	1
ρ_{HV}	0.96	0.985	1.1	1

Although the current results are based on equal weightings for all variables, the inclusion of a weighting parameter will allow future optimisation to account for the inclusion of more categories into the fuzzy scheme, as well as adjustment for variable signal quality of the four returns. The next set to be developed will be the detection of insects and other biological scatterers, which were commonly used to detect sea breezes during COPE.

4. Results

Once ground clutter had been identified using the fuzzy logic scheme, it was used to set these regions to no returns prior to the calculation of new QPE for the COPE period, the results of which are presented here. Figure 5 repeats the summation shown in Figure 4 with the filtered data. It clearly shows the benefits of the classification scheme, with a significant reduction in extreme accumulations.

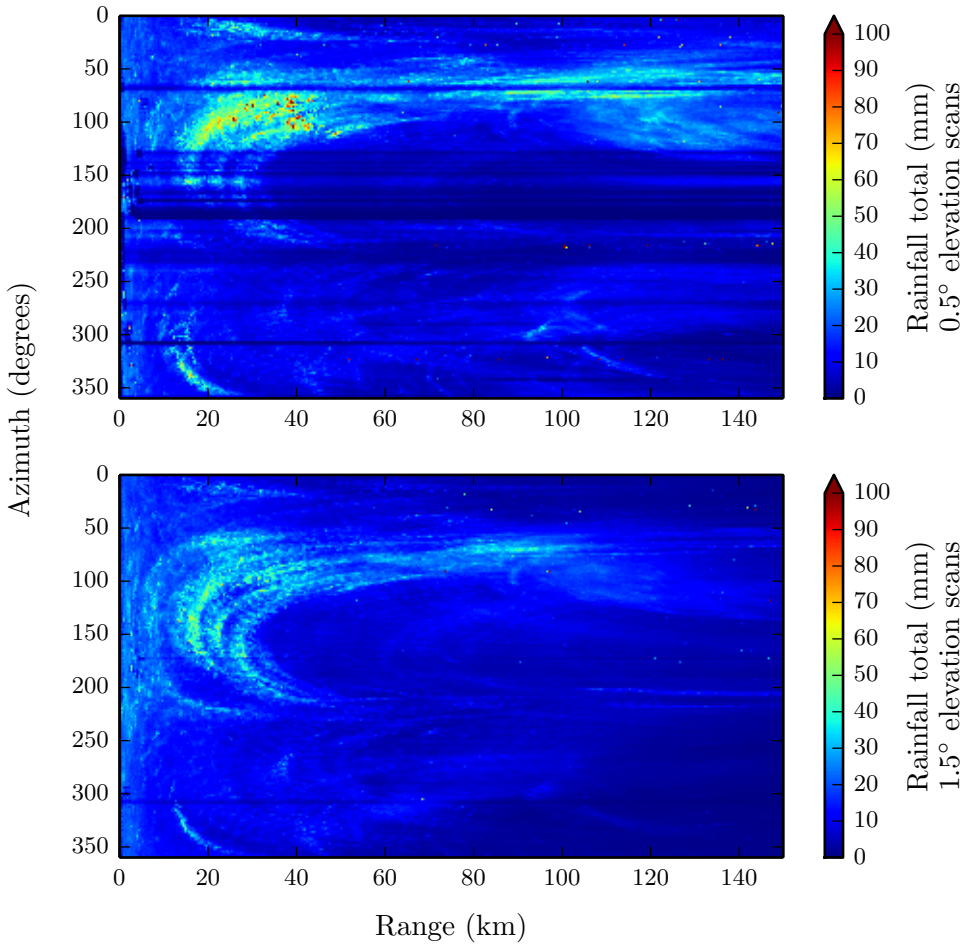

Figure 5: As figure 4 but rainfall totals calculated after the application of the fuzzy logic clutter filter. The maximum total for the 0.5° elevation is 1103.9mm and for the 1.5° elevation is 233.9mm.

Table 2: Rain gauge total rainfalls for COPE observation period.

Location	Rain Gauge Total (mm)	Raw Radar Total (mm)	Filtered Radar Total (mm)
Bodmin	10.6	7.6	7.5
Lanreath	23.4	8.0	6.0
Roadford	41.0	48.1	42.6
St Clether	18.8	243.9	9.2

Table 2 shows a few examples of the impact of the filter when comparing to rain gauge totals. The most significant change is seen for the St Clether rain gauge located 5.7km to the east of the radar, within the St Clether wind farm, which is the likely source of the anomalous returns. Several gauges show very minor change, indicating them to be largely free from AP and ground clutter errors. The gauges at Lanreath and Bodmin both show the counter effect of partial beam blockage, which remains in the data. This effect along with the improvement as a result of the clutter filter is summarised by Figure 6, which shows the dimensionally averaged rainfall totals pre and post filtering at 0.5° elevation. Averaging the data by range shows the impact of the near field clutter, out to 10km and also the impact of Dartmoor at 40km. After filtering these effects are removed, with the new profile reflecting the expected range decrease of radar derived accumulation as the beam widens and overshoots rainfall. In contrast the azimuthally averaged data is more interesting. The sharp spikes in the original data are a result of the local topography, including Dartmoor at 90-100 degrees. There is also strong evidence of partial beam blockage, which becomes more evident in the filtered data between 160 and 200 degrees and at 305 degrees. The underlying trend indicates an increase in accumulation inland, towards the higher topography in the East. Reproducing the statistics in Figure 2 with the new data yields a gradient of 0.40 and a correlation of 0.60, a small increase in performance, while the RMSE over all concurrent observations decreases from 0.825mm to 0.818mm.

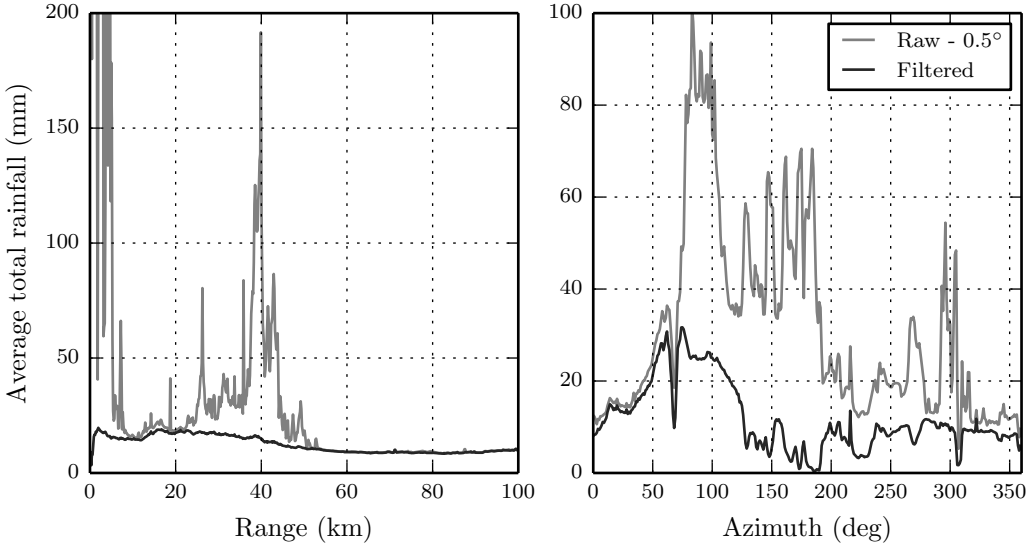

Figure 6: Range and radially averaged total rainfall totals for the COPE project. Grey lines show the original data, while black lines are after the application of the clutter filter. Both show the 0.5° elevation scan results.

5. Conclusions and future corrections

The use of an empirically derived fuzzy logic classification scheme to remove regions of anomalous propagation and ground clutter has improved the QPEs obtained from the NCAS radar, however it is clear that further corrections are required to produce a final product suitable for hydrological applications. Comparison with the limited coverage of rain gauges shows improvement for the St Clether gauge where clutter was an identifiable issue, while the wider summary statistics show a more representative field across the scan volume. The rain gauge time series will allow further analysis of the scheme for St Clether, to determine whether more information can be retrieved where rain is collocated with clutter.

The next stage in the radar processing chain will be to assess whether the data can be corrected for the beam blockage which is apparent in the lowest elevation scan, before applying dual polarisation variables to correct for attenuation resulting from intense rainfall. The ability to compare with both rain gauges and the C-band network will allow the improvement from each step of the process to be quantified.

Acknowledgement

We would like to thank all members of the COPE team, as well as the Dairy Crest Creamery and the Davidstow Airfield and Cornwall at War Museum for their logistical assistance during the campaign. We would also like to thank NERC for funding this work.

References

V. Chandrasekar, R. Keränen, S. Lim, and D. Moisseev, "Recent advances in classification of observations from dual polarization weather radars," *Atmospheric Research*, vol. 119, pp. 97–111, 2013.

C. Collier, A. Blyth, L. Bennett, D. Dufton, and J. French, "Polarimetric x-band radar measurements of the development of precipitation observed during cope," in *Extended Abstracts, 8th European Conf. on Radar in Meteorology and Hydrology, Garmisch-Partenkirchen*, 2014.

B. Dolan and S. A. Rutledge, "A theory-based hydrometeor identification algorithm for x-band polarimetric radars," *Journal of Atmospheric and Oceanic Technology*, vol. 26, no. 10, pp. 2071–2088, 2009.

U. Germann, G. Galli, M. Boscacci, and M. Bolliger, "Radar precipitation measurement in a mountainous region," *Quarterly Journal of the Royal Meteorological Society*, vol. 132, no. 618, pp. 1669–1692, 2006.

J. J. Gourley, P. Tabary, and J. Parent du Chatelet, "A fuzzy logic algorithm for the separation of precipitating from nonprecipitating echoes using polarimetric radar observations," *Journal of Atmospheric and Oceanic Technology*, vol. 24, no. 8, pp. 1439–1451, 2007.

D. Harrison, S. Driscoll, and M. Kitchen, "Improving precipitation estimates from weather radar using quality control and correction techniques," *Meteorological Applications*, vol. 7, no. 02, pp. 135–144, 2000.

J. S. Marshall and W. M. K. Palmer, "The distribution of raindrops with size," *Journal of Meteorology*, vol. 5, no. 4, pp. 165–166, 1948.

G. Villarini and W. F. Krajewski, "Review of the different sources of uncertainty in single polarization radar-based estimates of rainfall," *Surveys in Geophysics*, vol. 31, no. 1, pp. 107–129, 2010.